

Modelling of the toughening mechanisms in rubber-modified epoxy polymers

Part I *Finite element analysis studies*

Y. HUANG*, A. J. KINLOCH

Department of Mechanical Engineering, Imperial College of Science, Technology and Medicine, Exhibition Road, London SW7 2BX, UK

The finite element method has been employed to study the micromechanics and micromechanisms in rubber-toughened cross-linked-epoxy polymers. A two-dimensional plane-strain model has been proposed and has successfully been used to identify the stress fields associated with the dispersed rubbery phase and to simulate the initiation and growth of localized plastic shear-bands running between the rubbery particles. The effects of the microstructure and mechanical properties of the multiphase polymer on the nature and magnitude of the stress fields have also been examined.

1. Introduction

Single-phase epoxy polymers are usually relatively brittle materials and are frequently toughened by the incorporation of a rubbery phase [1]. Two important toughening mechanisms have been identified for such two-phase materials which consist of a rubbery phase dispersed in a matrix of a cross-linked polymer. The first is localized shear yielding, or shear banding, which occurs between rubber particles at an angle of approximately $\pm 45^\circ$ to the direction of the maximum principal tensile stress [1–3]. Owing to the large number of particles involved, the volume of thermoset matrix material which can undergo plastic yielding is effectively increased compared to the single-phase polymer. Consequently, far more irreversible energy dissipation is involved and the toughness of the material is improved. The second mechanism is the internal cavitation, or interfacial debonding, of the rubbery particles which then enables the subsequent growth of the voids so-formed by plastic deformation of the epoxy matrix [4, 5]. This irreversible hole-growth process of the epoxy matrix also dissipates energy and so contributes to the enhanced fracture toughness.

Obviously, when a second phase is introduced into an originally homogeneous matrix, it will cause stress concentrations around the secondary phase, be it a hard particulate inclusion, a rubbery particle, or a void. Stress concentrations will become even more significant when the volume fraction of the second phase is high, because there will be a strong interaction between the stress fields of neighbouring particles, or voids. Because plastic deformation will initiate from these stress concentrations, it is necessary to quantify the nature and magnitude of such stress fields in order to elucidate the mechanisms involved.

The simplest case to consider is a single particle embedded in an infinite isotropic matrix subjected to uniaxial tension. Goodier's analytical solution [6] may be applied to this problem. For a particle softer than the glassy matrix, the maximum principal stress is at the equator of the particle and the maximum stress concentration is approximately 1.8. In typical rubber-modified polymers, however, the stress fields associated with nearby rubbery particles will overlap and Goodier's solution is no longer applicable, unless the rubbery volume fraction is sufficiently low that this effect may be neglected. The effects of this stress field overlapping will obviously become more important when the particle volume fraction is high.

To analyse accurately the stress field, it is necessary to employ numerical methods such as the finite element method. The first study of rubber-modified polymers, which used an elastic analysis, was reported by Broutman and Panizza [7]. They simplified the two-phase material into an assembly of axisymmetric cells. Their study revealed that the maximum direct and shear stresses were located at the equator of the particle, indicating that yielding of the matrix would initiate from this point. They also found that the stress concentration increased in size as the volume fraction of rubbery particles was increased.

Agarwal and Broutman [8] developed a three-dimensional model to simulate the packing in a rubber-modified material. The results from assuming elastic behaviour using such a model were compared with the previous results obtained from employing the axisymmetric analysis. The two sets of results were found to agree well when presented as a function of inter-particle spacing. Because a three-dimensional analysis was more complicated, and more costly in

* Present address: National Power TEC, Kelvin Avenue, Leatherhead, Surrey KT22 7SE, U.K.

terms of computer resources, the authors subsequently concluded that the axisymmetric model could be used without a significant loss in accuracy.

In a recent study, a spatial statistical technique was incorporated into the axisymmetric model by Guild and Young [9] to study the influence of particle distribution on stress states around rubber particles. Their study suggested that particle distribution does not significantly change the calculated stress states around rubber particles when the rubbery volume fraction is below 0.3, which is usually the upper limit in rubber-toughened epoxy polymers [1].

It should be noted that all of the above-mentioned analyses were essentially elastic in nature. As a result, none of them could correctly predict the initiation and propagation of localized shear yielding (i.e. plastic shear bands). To achieve such a goal a truly elastic-plastic analysis must be conducted. In one of the few analyses where plasticity was taken into account, Haward and Owen [10] studied the problem of craze formation in glassy polymers. They employed a two-dimensional cylindrical void model subjected to uniaxial and biaxial loading conditions. Both the simple assumption of perfect elastic-plastic behaviour and the more complex material behaviour of strain-softening followed by strain-hardening were considered, and the plastic zone growth around the cavity was modelled. The stress to form a craze was found to be below the measured tensile yield stress of the glassy polymer. They concluded that groups of voids were more easily formed than isolated voids, due to interactions of the stress fields. However, no details of the shear-stress fields around these voids were given by the authors.

More recently, Sue and Yee [11] analysed the deformation behaviour of a polycarbonate plate with a circular hole. They experimentally observed that shear bands initially formed at the equator of the hole and then gradually shifted around the interface, towards the poles of the particles, before finally being localized into four shear bands which were about $\pm 45^\circ$ to the direction of the applied tensile stress,

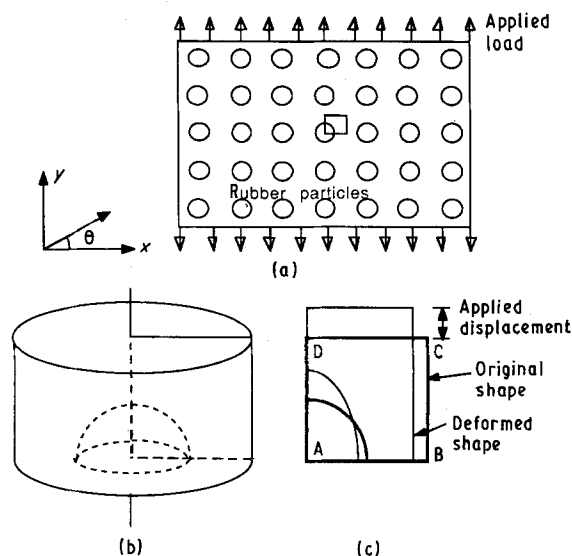


Figure 1 The axisymmetric model: (a) the packing of the particles; (b) the selected cylinder; (c) the boundary conditions.

initiating from the particle interface at about half-way between the equator and poles of the particle. Using an elastic-plastic finite element analysis, they demonstrated that the maximum octahedral shear stress did indeed also shift from the equatorial region of the hole towards the polar region. However, from the theoretical stress contours they obtained, there was no indication of any localization of the shear yielding process.

In the present paper, first an elastic and then an elastic-plastic analysis will be conducted using the conventional axisymmetric model to predict the deformation behaviour of rubber-modified epoxy polymers. It will be shown that such models cannot correctly predict the localized plastic deformation which is observed to occur. A new two-dimensional model will then be developed to simulate the plastic growth of shear bands. The effects of the microstructure and mechanical properties of the dispersed rubbery phase on the stress states will also be discussed. All the calculations were conducted using a VAX 8600 mainframe computer with the PAFEC [12] and the ABAQUS [13] commercial finite element packages. PAFEC is simple to use and has excellent graphical facilities, while ABAQUS is more powerful with respect to the non-linear analyses.

2. The axisymmetric model

2.1. Elastic analysis

The axisymmetric model simulates the multiphase material as a doubly periodically arranged array of cylinders, each of the cylinders containing a rubbery particle. Owing to periodical symmetry, only half of the cylinder is needed for analysis, as shown in Fig. 1. Mathematically, only a two-dimensional structure needs to be analysed, as illustrated in Fig. 1c. The boundary conditions were prescribed by: (i) a displacement being applied on boundary CD, (ii) boundary BC being kept parallel to its original shape, while (iii) boundaries AB and AD were constrained in the Y and X directions, respectively. The average applied stress σ_0 , was calculated from the reaction forces of the nodes on boundary CD. The Young's modulus was then calculated as

$$E = \sigma_0 / \varepsilon_0 \quad (1)$$

where ε_0 is the applied strain defined by

$$\varepsilon_0 = \ln(l/l_0) \quad (2)$$

where l_0 and l are the original and the deformed lengths of boundary BC, respectively. A typical finite element mesh used in the present study is shown in Fig. 2. Eight-noded quadrilateral isoparametric elements were used for the epoxy matrix, whereas six-noded triangular elements were used for the rubbery particle. This enabled an automatic mesh to be readily generated.

Distributions of the direct stress, σ_{yy} , and the equivalent or von Mises stress, σ_{vm} , are presented in Fig. 3a and b, respectively. The von Mises stress is defined by

$$(\sigma_1 - \sigma_2)^2 + (\sigma_2 - \sigma_3)^2 + (\sigma_3 - \sigma_1)^2 = 2\sigma_{vm}^2 \quad (3)$$

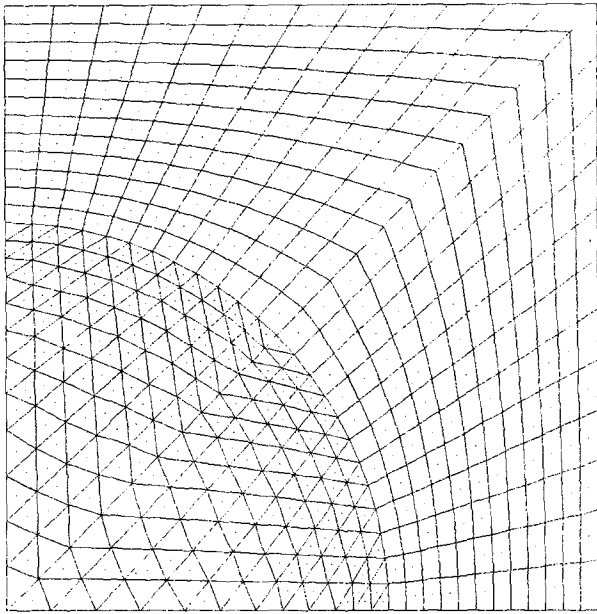


Figure 2 A typical finite element mesh employed for the axisymmetric model.

where σ_1 , σ_2 and σ_3 are the three principal stresses.

The maxima of both the direct and the von Mises stresses in the matrix were found to be at the equator of the particle, confirming previous reports by other authors [7-9]. The maximum stress concentration factors for the direct and the von Mises stresses were denoted K_{yy} and K_{vm} and may be calculated from

$$K_{yy} = (\sigma_{yy})_{\max}/\sigma_0 \quad (4)$$

and

$$K_{vm} = (\sigma_{vm})_{\max}/\sigma_0 \quad (5)$$

Table I shows calculated results for a rubber-modified epoxy, which was obtained by blending 15 p.h.r. rubber and 5 p.h.r. piperidine with 100 p.h.r. epoxy resin and by curing the mixture at 160 °C for 6 h [4, 14] (p.h.r. stands for "parts per hundred resin"). The elastic modulus of the epoxy matrix was measured to be 3.2 GPa [4] and its Poisson's ratio was assumed to be 0.35. The elastic modulus for the rubber was taken to be 2 MPa [15] and its Poisson's ratio was assumed to be 0.49. These values for the mechanical properties for the rubbery and the epoxy phases will be used in all the calculations throughout this paper, unless otherwise stated.

Now internal cavitation of the rubbery particles or debonding of the particles from the matrix leads to voids (cavities) being formed [1]. By neglecting any plastic void growth at this stage, the void can be treated as a particle with zero modulus, and a similar analysis to that described above was therefore conducted to calculate the stress concentration factors around the voids and the Young's moduli of the voided epoxy polymer. The results are also shown in Table I. Obviously, the formation of voids due to the internal cavitation of the rubbery particles or debonding of the particles from the matrix does not significantly change the level of the stress concentrations in the epoxy matrix. Further, the stress contours are not significantly affected by the cavitation

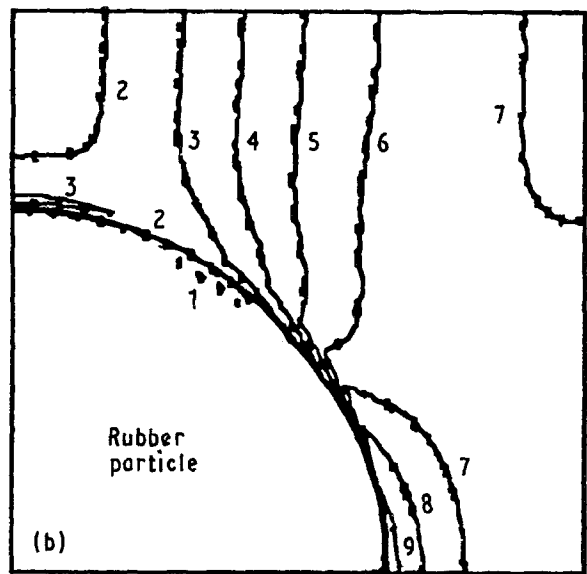
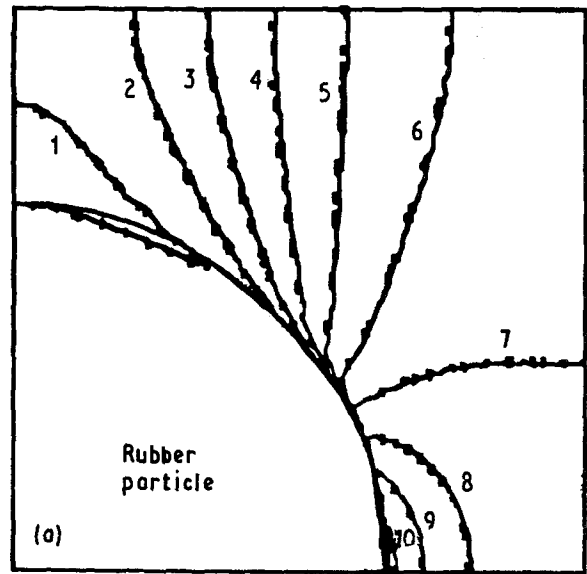


Figure 3 (a) Distribution of direct stress, σ_{yy} , at an applied strain of 0.001. (b) Distribution of the von Mises stress, σ_{vm} , at an applied strain of 0.001. (Axisymmetric model; elastic analysis.) 1, 0.00; 2, 0.56; 3, 1.11; 4, 1.66; 5, 2.22; 6, 2.77; 7, 3.33; 8, 3.88; 9, 4.44; 10, 5.00.

TABLE I The mechanical properties of the rubber and epoxy phases used for calculating the elastic stress concentration factors

Phase	Volume fraction	E_e (GPa)	ν_e	E_r (MPa)	ν_r	K_{yy}	K_{vm}
Rubber	0.19	3.2	0.35	2.0	0.49	2.43	2.21
Void	0.19	3.2	0.35	-	-	2.43	2.22

E = Young's modulus; ν = Poisson's ratio; e, epoxy; r, rubber; ν_r rubber = 0.19; elastic analysis.

of rubbery particles, as may be seen by comparing Figs 3b and 4.

2.2. Elastic-plastic analysis

An elastic-plastic analysis has also been conducted using the axisymmetric model. This will represent the actual condition near a crack tip more closely, because there is always plastic yielding in this region [16]. It is also a necessary requirement if the formation of a

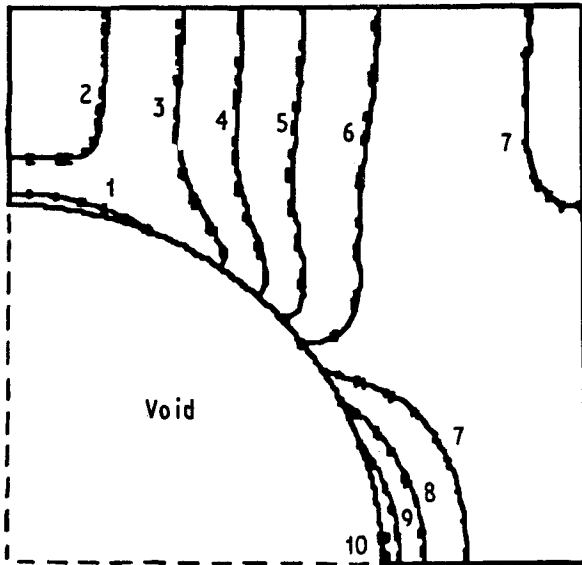


Figure 4 The distribution of the von Mises stress, σ_{vm} , around a void at an applied strain of 0.001. (Axisymmetric model; elastic analysis.) 1, 0.00; 2, 0.56; 3, 1.11; 4, 1.66; 5, 2.22; 6, 2.77; 7, 3.33; 8, 3.88; 9, 4.44; 10, 5.00.

localized yield zone (i.e. plastic shear band) is to be modelled.

The same mesh was employed as previously used in the elastic analysis. A piecewise stress versus strain curve was employed to model the constitutive property of the epoxy matrix, as illustrated in Fig. 5. This stress versus strain curve was derived from an experimentally determined stress–strain curve for an unmodified epoxy polymer [4], which is also shown in Fig. 5. The experimental curve in Fig. 5 was obtained by scaling a compressive stress versus strain curve by a factor of 0.75, due to the differences in the tensile and compressive yield stresses [17]. It should be noted that there is stress softening after yielding, which is common for most glassy polymers and is a necessary condition for localized shear bands to occur [18]. It is followed by a plateau before the material strain hardens.

As predicted from the elastic analysis, the plastic zone first initiated around the equator of the void when the applied stress reached a critical level, as illustrated in Fig. 6a where the parameter shown in the contour plot is the equivalent plastic strain. It should be noted that no rubber particle is present in Fig. 6, because it was experimentally observed that for the material being modelled in the present study the rubbery particles cavitated when the applied strain reached the yield strain of the epoxy matrix [4]. Now the results shown in Fig. 6a–d clearly reveal that the plastic zone grows steadily in size as the applied displacement is increased. Also, when the applied strain reached about 0.3, the maximum strain in the epoxy reached the experimentally measured fracture strain of the matrix epoxy, which was determined to be about 0.71 using a plane–strain compression test [4]. Fracture of the material may be assumed to occur at this stage. However, from examining Fig. 6, it is obvious that the yield zone does not localize to give a clearly defined plastic shear band. Thus, the axisym-

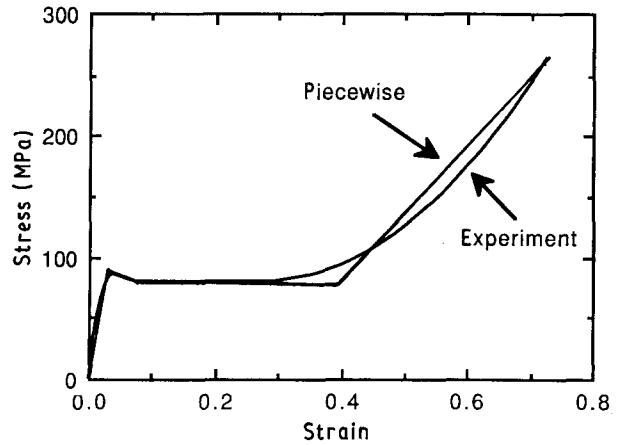


Figure 5 The experimental and the simplified piecewise tensile stress versus strain curve for the epoxy matrix.

metric model cannot simulate the process of localized shear yielding in the fracture of the rubber-toughened epoxies, which is one of the main toughening mechanisms.

3. The two-dimensional plane-strain model

3.1. Introduction

In order to model the localized plastic shear-banding process in the deformation of the rubber-modified epoxies, a new two-dimensional plane-strain model has been developed, which is shown in Fig. 7. The particles in this model are arranged in a different manner compared to the axisymmetric model which is shown in Fig. 1. Due to this change, the basic element which can be singled out to represent the multiphase material is different from the axisymmetric model, as is also illustrated in Fig. 7. The boundary conditions were prescribed as follows:

$$\begin{aligned} (u_y)_{AB} &= -(u_y)_{CD} \\ &= -u_0/2 \end{aligned} \quad (6)$$

$$(u_x)_{AD} = -(u_x)_{BC} \quad (7)$$

where u_0 is the prescribed displacement. These two conditions were required by the periodical symmetry of the structure. Obviously, in this model, the stress field of one particle mainly interacts with those of the four neighbouring particles which lie in the direction of $\pm 45^\circ$ to the direction of the applied stress. Also, the proposed model may better represent the stress state ahead of a crack tip, because it is then a global plane-strain fracture which is generally under examination.

3.2. Elastic analysis

The computing procedures were similar to those described in the last section. The typical mesh employed in the analysis is shown in Fig. 8, and Fig. 9 shows the contours of the direct stress, σ_{yy} , and the von Mises stress, σ_{vm} . As was observed for the elastic analysis using the axisymmetric model, the maxima for the direct and the von Mises stresses still occur at the equator, indicating that the growth of the plastic zone

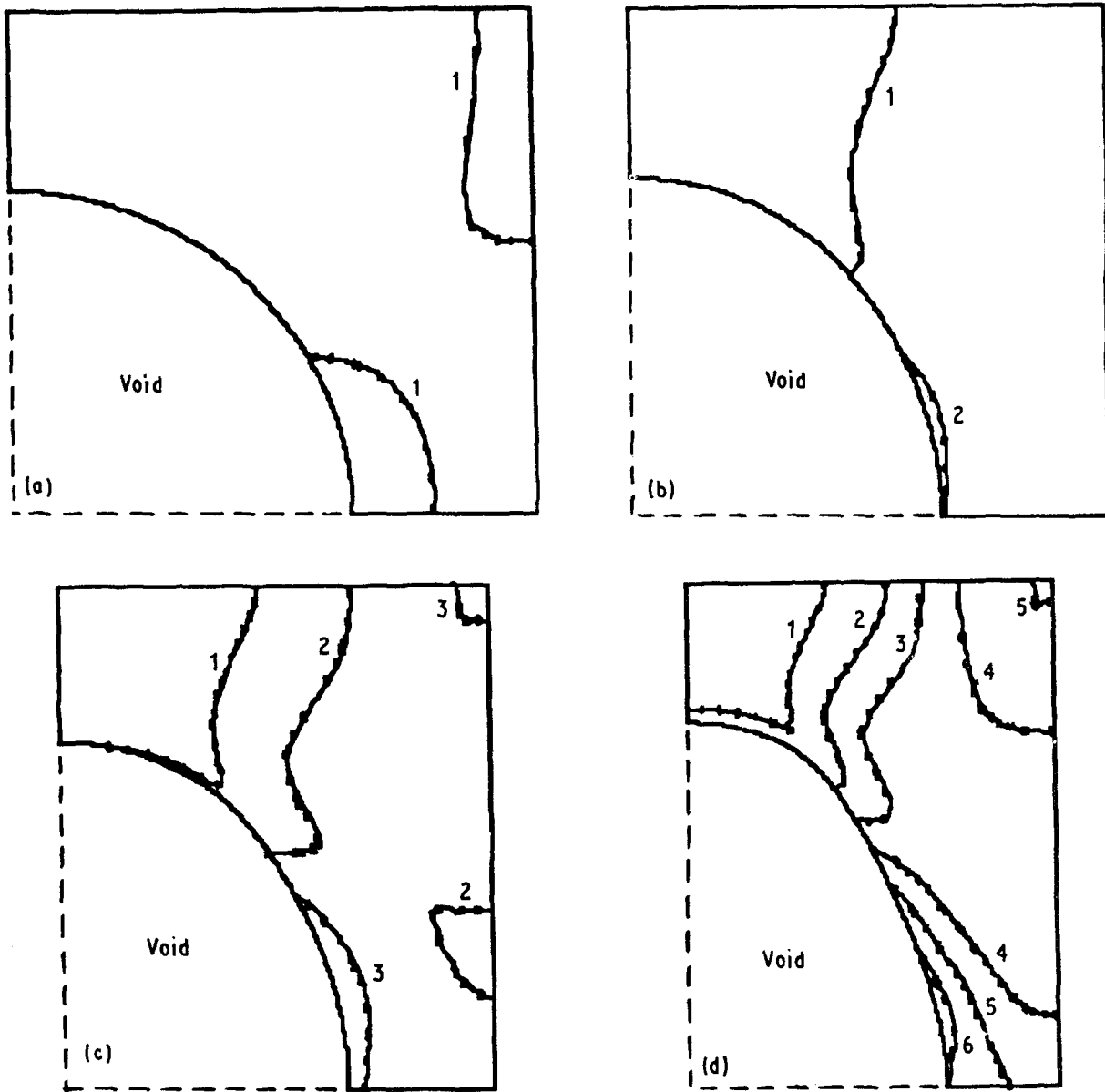


Figure 6 Predicted growth of the plastic yield zone at different stages of loading using the axisymmetric model. Applied strain: (a) 0.035; (b) 0.075; (c) 0.150; (d) 0.300. (Elastic-plastic analysis.) Equivalent plastic strain: 1, 0.010; 2, 0.087; 3, 0.163; 4, 0.240; 5, 0.316; 6, 0.393; 7, 0.470; 8, 0.546; 9, 0.623; 10, 0.700.

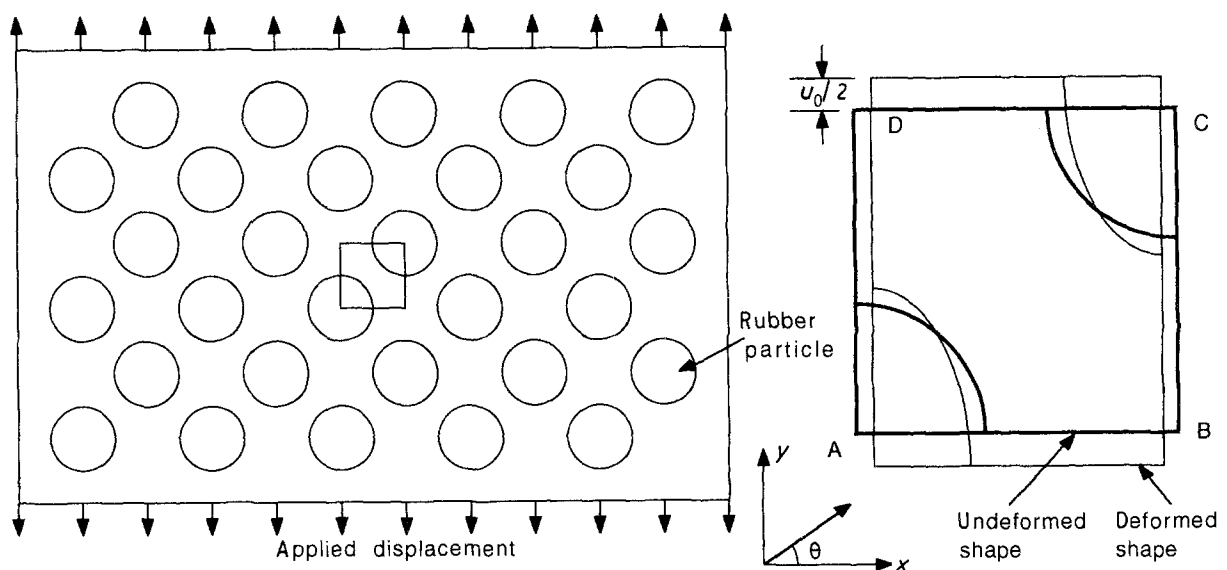


Figure 7 The two-dimensional plane-strain model for the rubber-modified epoxy under tensile loading.

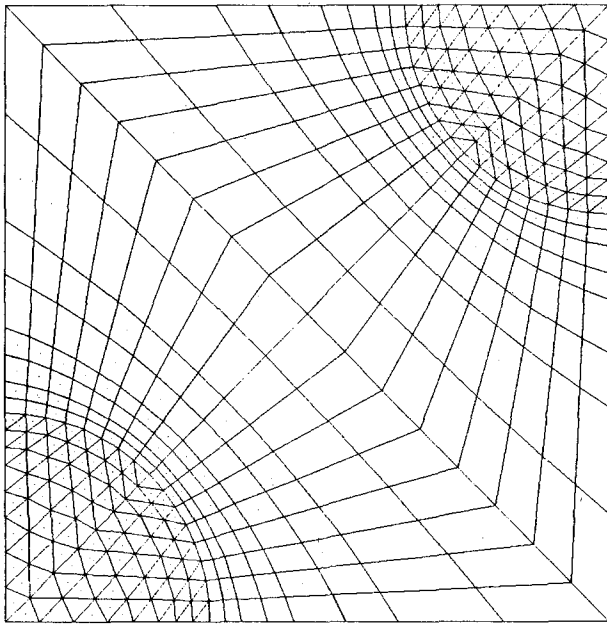


Figure 8 A typical finite element mesh employed for the two-dimensional plane-strain model.

will initiate from the equatorial regions. Table II compares the results calculated from the present two-dimensional model and the axisymmetric model. As may be seen, the stress concentration factors predicted by the new model are about 75% higher than those deduced using the axisymmetric model, although the only difference between these two models is the manner in which rubber particles are arranged. However, this difference is not unexpected because the stress concentration factor is highly dependent on the interactions between the stress fields of the neighbouring particles. Obviously, the interactions will be strongly influenced by the arrangement of the particles. The above calculation suggests that the arrangement in the new model has actually increased such interactions. Further, from Fig. 9b it is clear that the von Mises stress is much higher in the region along one of the diagonal lines which connects the centres of the two particles. The indication from this figure is that after the initiation of a plastic zone in the equatorial region, further plastic deformation will localize along this line, which is inclined 45° to the direction of the applied stress. This is discussed further in the next section when an elastic-plastic analysis is undertaken.

Again, if the effect of cavitation is modelled, then the cavitation of rubber particles, or the debonding of the particle from the epoxy matrix, does not cause significant changes in the stress distributions in the epoxy matrix. For example, Fig. 10, which shows the distribution of the von Mises stress around the cavity, is very similar to the stress contour in Fig. 9b. This issue will be further discussed later when the effects of the mechanical properties of rubber particles on the stress distribution in the epoxy matrix are investigated.

3.3. Elastic-plastic analysis

The constitutive relationship for the matrix material has been shown in Fig. 5 and, as previously noted, stress softening and strain hardening of the epoxy

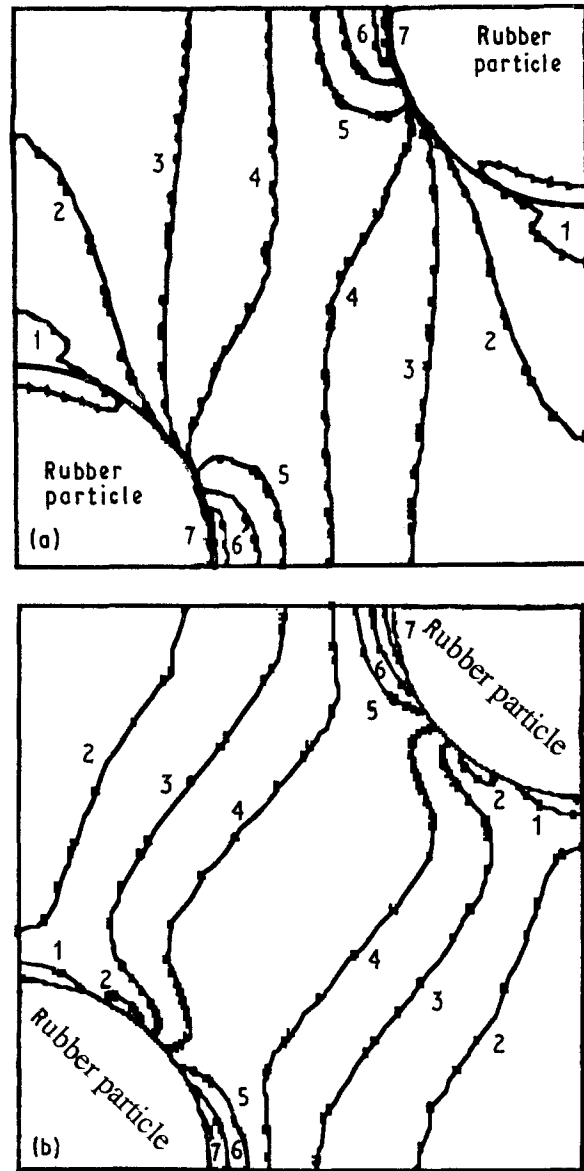


Figure 9 (a) Distribution of direct stress, σ_{yy} , at an applied strain of 0.002. (b) Distribution of the von Mises stress, σ_{vm} , at an applied strain of 0.002. (Two-dimensional plane-strain model; elastic analysis.) (a) σ_{yy} (MPa): 1, 0.00; 2, 2.22; 3, 4.44; 4, 6.67; 5, 8.89; 6, 11.1; 7, 13.3; 8, 15.5; 9, 17.7; 10, 20.0; (b) von Mises stress (MPa): 1, 0.00; 2, 1.22; 3, 2.44; 4, 3.66; 5, 4.88; 6, 6.11; 7, 7.33; 8, 8.77; 9, 9.77; 10, 11.0.

TABLE II Comparison of the predicted maximum elastic stress concentrations around the rubbery particles

Model	K_{yy}	K_{vm}
Axisymmetric model	2.43	2.21
Two-dimensional plane strain model	4.36	3.81

Material properties: epoxy, $E = 3.2$ GPa, $\nu_e = 0.35$, rubber $E = 2.0$ MPa, $\nu_r = 0.49$, ν_t rubber = 0.19; elastic analysis.

matrix has been incorporated, especially as the former is a necessary condition for shear banding to occur [18]. As shown in Fig. 11a-d, when the applied displacement reached 0.025, a plastic zone starts to develop at the equator. Now, as the applied displacement is further increased, then the location of the maximum equivalent plastic strain moves from the equator towards the pole (cf. Fig. 11a and b) and a plastic yield zone gradually develops along the intersecting line of the two particles. Finally, a band of

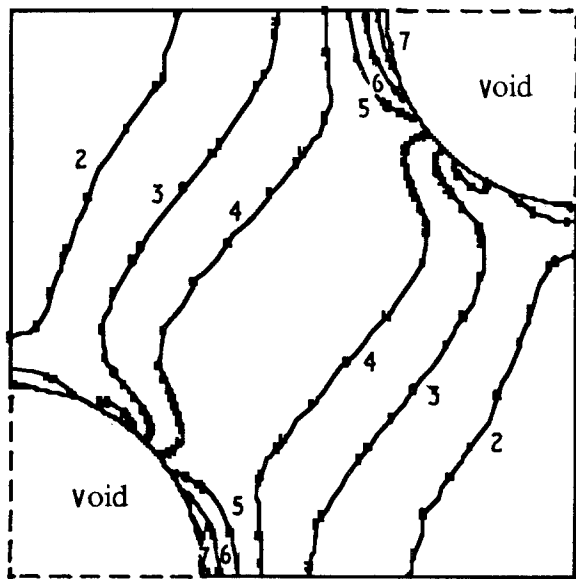


Figure 10 Distribution of the von Mises stress, σ_{vm} , around a cavity at an applied strain of 0.002. (Two-dimensional plane-strain model; elastic analysis.) von Mises stress (MPa): 1, 0.00; 2, 1.22; 3, 2.44; 4, 3.66; 5, 4.88; 6, 6.11; 7, 7.33; 8, 8.77; 9, 9.77; 10, 11.0.

plastic deformation is formed along the diagonal line linking the two voids. Plasticity was highly localized in this band even when the applied displacement was further increased. When the applied strain reached about 0.1, the maximum strain in the band reached the fracture strain of the matrix material, which has a value of 0.71, as measured from a plane-strain compression test [4]. Again in these plots, no rubber particles are present because they have already cavitated at the beginning of yielding. Clearly, once the band is formed, further yielding is localized inside the band until fracture occurs. Thus, the present model successfully predicts the formation and growth of localized shear bands in the deformation of rubber-toughened glassy polymers.

It should be noted from these contours, and from Fig. 7, that the structure under analysis is antisymmetric. Mathematically, it is therefore feasible to analyse only half of the structure. However, the full structure was employed in order to study the growth of a complete shear band between two rubber particles.

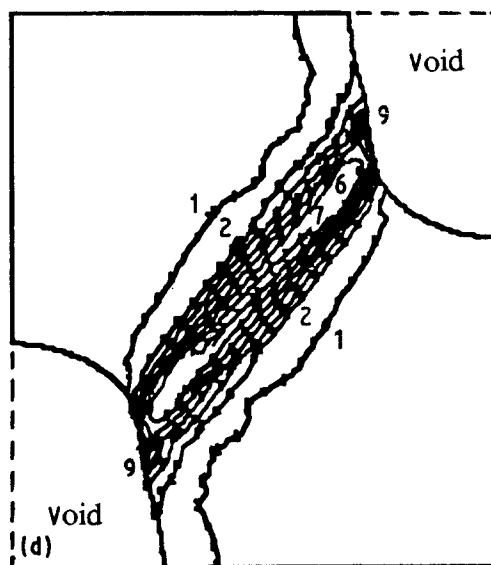
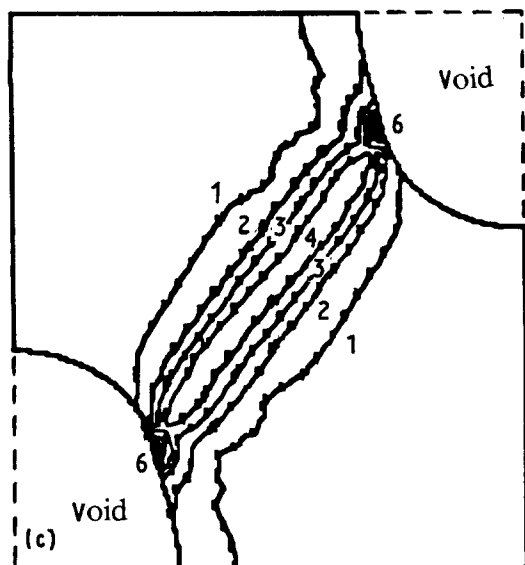
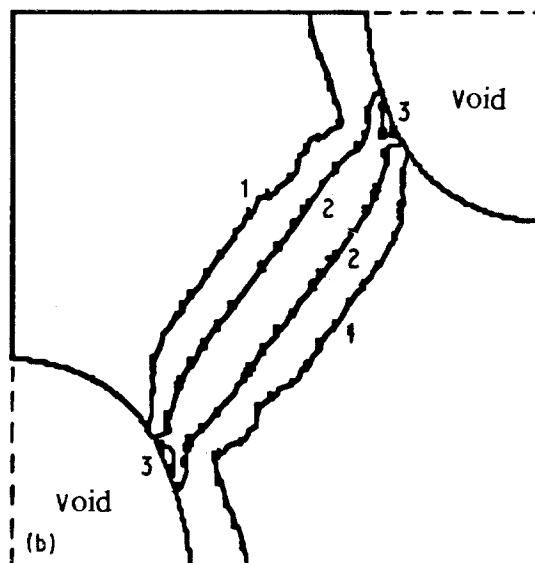
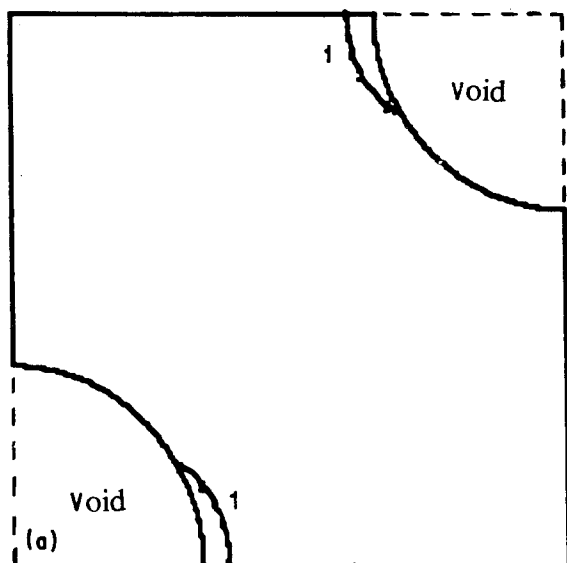


Figure 11 Predicted growth of the plastic yield band at different stages of loading using the two-dimensional plane-strain model. Applied strain: (a) 0.025; (b) 0.050; (c) 0.075; (d) 0.100. (Elastic-plastic analysis.) Equivalent plastic strain: 1, 0.010; 2, 0.087; 3, 0.163; 4, 0.240; 5, 0.316; 6, 0.393; 7, 0.470; 8, 0.546; 9, 0.623; 10, 0.700.

4. The critical applied stress

Two stress concentration factors, K_{yy} and K_{vm} , have been defined in Equations 4 and 5. The former refers to the concentration of the direct stress and the latter to the concentration of the von Mises stress, compared to the average applied stress. The concentration factor of the von Mises stress, K_{vm} , is worthy of further discussion. Because the stress field around the particle is triaxial, the uniaxial yield stress is no longer a suitable parameter to use as the yield criterion. Instead, the von Mises yield criterion or the Tresca yield criterion should be used [16, 18]. In the present analysis, the von Mises criterion was chosen and yield was assumed to occur when the von Mises stress, σ_{vm} , reached the value of the uniaxial yield stress of the matrix material. However, because the stress field around the particle was not uniform, microscopically, yield will occur when the maximum von Mises stress attains the value of the uniaxial yield stress. The average applied stress at this state is termed the critical applied stress for the material, σ_c , and was defined by Broutman and Panizza [7]. It may be related to the uniaxial yield stress, σ_y , by the following equation

$$\begin{aligned}\sigma_c &= \sigma_0 \frac{\sigma_y}{(\sigma_{vm})_{\max}} \\ &= \frac{\sigma_y}{K_{vm}}\end{aligned}\quad (8)$$

The above equation suggests that, due to the incorporation of rubbery particles, the applied stress at which yield occurs is reduced by a factor K_{vm} . It is this factor which will be used in the development of a mathematical model to predict quantitatively the toughening induced by the rubbery particles in Part II of the present work [19].

It should be noted that the critical stress as defined above is different from the bulk yield stress of the multiphase rubber-modified epoxy. When the applied stress is at the critical stress, yielding occurs near the equators of the rubbery particles or voids. However, the multiphase rubber-toughened epoxy may behave macroscopically in a linear elastic manner. In other words, the critical stress is the effective yield stress which characterizes the formation of a plastic zone in multiphase polymers. The calculation of the size of plastic zone by the Irwin model should then be modified for the multiphase materials as

$$r_y = (K_I/\sigma_c)^2/6\pi \quad (9)$$

Recently, Mauzac and Schirrer [20] have also proposed a similar modification to the Irwin model in their study of crack-tip damage zones in rubber-toughened polymers. They proposed a "damage initiation threshold stress", σ_{th} , which is essentially the same as the critical applied stress defined in Equation 8.

5. Microstructural and mechanical property effects

5.1. Effects of dispersed rubbery phase volume fraction

The rubbery volume fraction has been shown [1] to be

one of the most important microstructural parameters in determining the fracture properties of rubber-toughened epoxies. Fig. 12 compares the experimental values of the elastic moduli for a rubber-modified epoxy [21] with the numerical predictions using the two-dimensional plane-strain model. Obviously, when the rubbery volume fraction is within the range 0.0–0.2, the predictions are in reasonable agreement with experimental values. The agreement is particularly good considering the fact that the modulus and the Poisson's ratio of the rubber used in the calculations were only estimates. Beyond a volume fraction of about 0.2, there are no experimental data available for comparison, because when higher concentrations of rubber are used, phase inversion of the multiphase polymer normally occurs [1].

With the increase in rubbery volume fraction, the concentration of the von Mises stress will increase due to the increased interaction between the stress fields of nearby rubber particles, as demonstrated in Fig. 13. However, predictions from the two-dimensional plane-strain model are significantly higher than that from the axisymmetric model. As pointed out earlier,

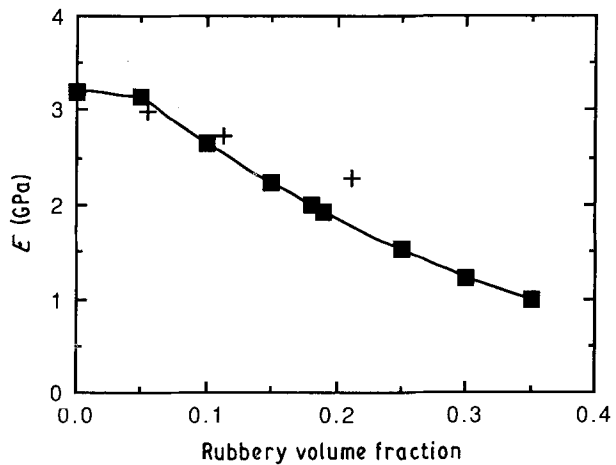


Figure 12 Comparison between the calculated Young's modulus of the multiphase polymer and the experimental values. (Two-dimensional plane-strain model; elastic analysis.) (■ numerical; + experiment)

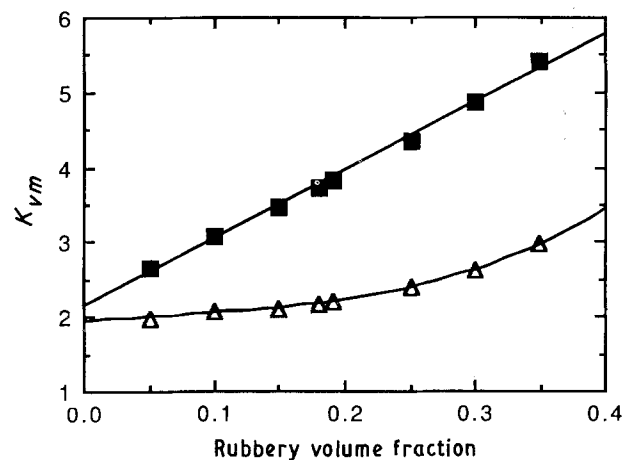


Figure 13 Calculated von Mises stress concentration factor, K_{vm} , as a function of volume fraction of the dispersed rubbery phase. (■ Two-dimensional plane-strain model; Δ axisymmetric model; both elastic analysis.)

the arrangement of the particles in the former model maximizes the interaction between their stress fields and results in the higher stress concentration factor. Further, it should be noted that when the axisymmetric model is employed, the maximum von Mises stress increases relatively slowly with volume fraction over the range of volume fractions up to about 0.3. The two-dimensional plane-strain model, on the other hand, predicts a steady rise in the von Mises stress concentration with rubbery volume fraction, and an approximate linear relationship exists. Thus, the two-dimensional plane-strain model predicts that the extent of shear yielding will be enhanced steadily by an increase in the rubbery volume fraction. For rubber-toughened thermosetting polymers this prediction is in better agreement with many experimental observations which have shown that the fracture toughness of rubber-modified epoxy polymers does indeed increase steadily with an increase in the rubbery volume fraction [1]. The differences between the two models most probably arise from the different arrangements of particles and degrees of constraint which are assumed.

In addition to the rubbery volume fraction, the mechanical properties of the epoxy matrix and rubbery particles may also have a strong influence on the stress fields in and around the rubbery particles. These are considered in the following section.

5.2. Effect of rubber modulus

Fig. 14 shows predictions from the two-dimensional plane-strain model for the Young's modulus (Fig. 14a) of the multiphase rubber-toughened epoxy and the maximum von Mises stress concentration factor (Fig. 14b) as a function of $\log(E_e/E_r)$, where E_e and E_r are the Young's moduli of the epoxy and rubber, respectively. A rubbery volume fraction of 19% has been assumed. In the calculation, the Poisson's ratios of the epoxy and rubber were assumed to be 0.35 and 0.49, respectively, and the Young's modulus of the epoxy matrix was kept constant at a value of 3.2 GPa. Initially, the Young's modulus of the two-phase material decreases sharply with an increase in the value of $\log(E_e/E_r)$. When the value of $\log(E_e/E_r)$ reaches a value of about 3.0, it approaches a constant lower-bound value of about 1.82 GPa.

The von Mises stress concentration factor, on the other hand, increases steeply until $\log(E_e/E_r)$ reaches a value above 3.0, when a constant value of about 3.8 is attained. It should be noted that when E_e equals E_r , the von Mises stress concentration factor is slightly higher than unity, due to the differences in the Poisson's ratios of the two phases. The Young's moduli for the epoxy and the rubber are typically about 3.0 GPa and 2.0 MPa, respectively, which corresponds to a $\log(E_e/E_r)$ ratio of 3.18. Thus, with the above assumptions, the stress field around such a rubbery particle is not significantly different from that around a void, which corresponds to a $\log(E_e/E_r)$ ratio $\rightarrow \infty$. As a result, it can be concluded that the internal cavitation, or debonding of the rubber particles, does not cause any significant differences in the stress fields around the rubbery particles. It merely

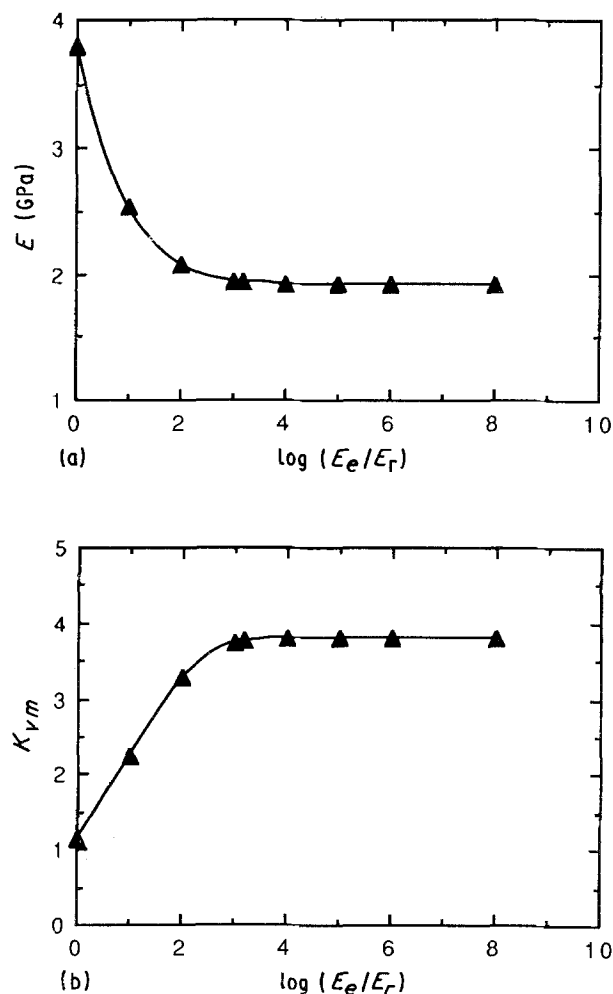


Figure 14 Calculated relationships between: (a) Young's modulus, E , of the rubber-toughened epoxy and the ratio of the moduli of the two phases; (b) von Mises stress concentration factor, K_{vm} , and the ratio of the moduli of the two phases. (Two-dimensional plane-strain model; elastic analysis.)

creates a void which may then grow further as a result of plastic deformation of the epoxy matrix [4, 5].

From the above results, it may also be concluded that the interfacial bonding between the dispersed rubbery particle and epoxy matrix is not important. This is in agreement with recent experimental observations by the authors [4]. It also agrees with a recent analysis by Liu and Nauman [22], who extended Goodier's solution to analyse the stress state inside a single inclusion in an infinite plate. However, the present analysis also has taken the interaction between particles (voids) into consideration and is therefore more applicable to rubber-modified thermosetting polymers.

5.3. Effect of Poisson's ratio of the rubbery particles

Fig. 15 shows the predictions from the two-dimensional plane-strain model for the maximum Mises stress concentration, K_{vm} , as a function of the Poisson's ratio, ν_r , of the rubbery phase. A volume fraction of dispersed rubbery phase of 0.19 has been assumed and the value of the ratio of $\log(E_e/E_r)$ has been taken to be 3.18. The value of K_{vm} is not significantly dependent upon the value of ν_r , until the value of

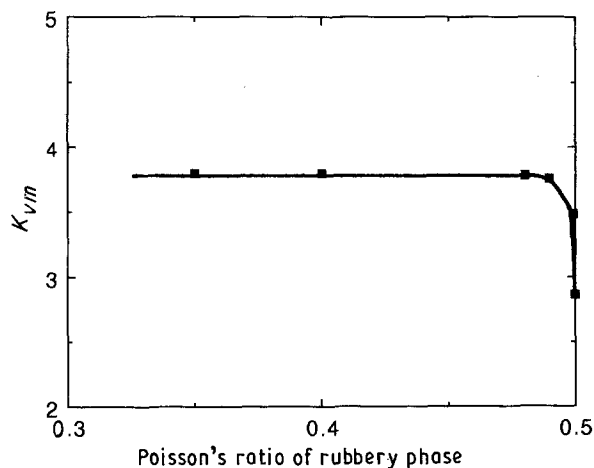


Figure 15 Calculated relationship between the von Mises stress concentration factor, $K_{v/m}$, and the Poisson's ratio, v_r , of the dispersed rubbery phase. (Two-dimensional plane-strain model; elastic analysis.)

v_r rises above about 0.49; when $v_r = 0.499$ the value of $K_{v/m}$ is 3.48 and when $v_r = 0.4999$ the value of $K_{v/m}$ is 2.86. Hence, to return to the question of the stress concentration associated with a void, a void may then actually generate a somewhat higher local stress concentration if the Poisson's ratio of the rubbery particle is significantly above about 0.49.

6. Conclusions

A two-dimensional plane-strain model has been developed to analyse the stress fields around the dispersed rubbery particles in multiphase rubber-modified epoxy polymers. The epoxy matrix has been modelled as either an elastic or elastic-plastic material. The investigation has revealed that the conventional axisymmetric model underestimates the effects of rubbery inclusions in creating stress concentrations inside the glassy polymeric matrix. Furthermore, the present model has been successfully applied to simulate the initiation and growth of the localized shear bands that have been observed to develop between rubbery particles or voids.

In Part II [19] of the paper the results given in the present paper will be extended to model quantitatively

the plastic shear band and plastic void-growth mechanisms. This will enable a detailed, predictive model to be developed for the toughening mechanisms induced by the presence of a dispersed rubbery phase in a thermosetting polymeric matrix.

Acknowledgements

The authors thank the British Council for providing a studentship to Y. Huang, and also Drs F. Guild and R. Fenner for helpful discussions on the work.

References

1. A. J. KINLOCH, in "Rubber-Toughened Plastics", edited by C. K. Riew, 'Advances in Chemistry Series' Vol. 222 (American Chemical Society, Washington, DC, 1989) p. 67.
2. A. J. KINLOCH, S. J. SHAW and D. L. HUNSTON, *Polymer* **24** (1983) 1355.
3. R. A. PEARSON and A. F. YEE, *J. Mater. Sci.* **21** (1986) 2475.
4. Y. HUANG, PhD Thesis, University of London (1991).
5. Y. HUANG and A. J. KINLOCH, *J. Mater. Sci. Lett.* (1992) in press.
6. J. N. GOODIER, *ASME Appl. Mech. Mag.* **55** (1933) 39.
7. L. J. BROUTMAN and G. PANIZZA, *Int. J. Polym. Mater.* **1** (1971) 95.
8. B. D. AGARWAL and L. J. BROUTMAN, *Fibre Sci. Tech.* **7** (1974) 63.
9. F. J. GUILD and R. J. YOUNG, *J. Mater. Sci.* **24** (1989) 2454.
10. R. N. HAWARD and D. R. J. OWEN, *ibid.* **8** (1973) 1136.
11. H. J. SUE and A. F. YEE, *Polymer* **29** (1988) 1619.
12. "PAFEC User's Manual", Level 6.2 (PAFEC 1988) (Nottingham, UK).
13. "ABAQUS User's Manual" (Habbit, Karlsson and Sorensen, 1988) (Pawtucket, RI, USA).
14. A. J. KINLOCH, C. A. FINCH and S. HASHEMI, *Polym. Commun.* **28** (1987) 229.
15. S. C. KUNZ and P. W. R. BEAUMONT, *J. Mater. Sci.* **16** (1981) 3141.
16. A. J. KINLOCH and R. J. YOUNG, "Fracture Behaviour of Polymers" (Applied Science, London, 1983).
17. A. S. WRONSKI and M. PICK, *J. Mater. Sci.* **12** (1977) 28.
18. P. B. BOWDEN, in "The Physics of Glassy Polymers", edited by R. N. Haward (Applied Science, London, 1975).
19. Y. HUANG and A. J. KINLOCH, *J. Mater. Sci.* **27** (1992) 2763.
20. O. MAUZAC and R. SCHIRRE, *J. Mater. Sci.* **25** (1990) 5125.
21. A. F. YEE and R. A. PEARSON, *ibid.* **21** (1986) 2462.
22. S. H. LIU and E. B. NAUMAN, *ibid.* **25** (1990) 2071.

Received 30 July

and accepted 2 August 1991